Data supplement for Cao et al., A Functional Connectome-Based Neural Signature for Individualized Prediction of Antipsychotic Response in First-Episode Psychosis. Am J Psychiatry (doi: 10.1176/appi.ajp.20220719)

Supplementary Methods

Sample details

Patients in the discovery and validation samples were recruited based on the DSM-IV diagnosis of a psychosis spectrum disorder. The discovery sample is a completely new dataset that has not been reported anywhere before, while the validation sample partly overlaps with the one used in Sarpal et al. (1). For both samples, the inclusion criteria were: 1) age between 15 and 40 years; 2) a score ≥ 4 (moderate) for any of the psychosis items in the BPRS-A; and 3) with minimal exposure to antipsychotic drugs for a cumulative lifetime period of less than two weeks. The exclusion criteria included: 1) serious neurological or endocrine disorders; 2) any medical conditions requiring medication with psychotropic effects; 3) significant risk of suicidal or homicidal behavior; 4) drug abuse or dependence; 5) cognitive or language limitations unable to sign an informed consent; and 6) contraindications to antipsychotic monotherapy or MRI scans. In the discovery sample, patients were randomized to receive open-label, naturalistic treatment with either risperidone or aripiprazole for 12 weeks (ClinicalTrials.gov ID: NCT02822092). In the validation sample, patients were randomized for double-blinded, single antipsychotic treatment (either risperidone or aripiprazole) for 12 weeks (ClinicalTrials.gov ID: NCT00320671). Patients started at low dosage and gradually increased to the target dosage at day 7 (3 mg risperidone or 15 mg aripiprazole daily). Depending on the relief of psychotic symptoms, subjects either stayed on the target dosage or continued to increase dosage after week 4 until reaching the maximal dosage of 6 mg risperidone or 30 mg aripiprazole daily. Except for these two drugs, no other antipsychotics, mood stabilizers, or antidepressants were allowed during the study. However, in case of need, benztropine and lorazepam were allowed to alleviate extrapyramidal symptoms, akathisia, and anxiety. The BPRS-A was performed at baseline, weeks 1, 2, 3, 4, 6, 8, 10, and 12. The SCID was conducted at baseline and the diagnosis was further confirmed at a diagnostic consensus meeting where cases were presented after participants completed the 12 weeks of the study. The fMRI scans were conducted at baseline before medication. In the discovery sample, 36 out of 49 participants completed 12-week follow-ups, with the rest having at least one follow-up assessment. In the validation sample, 18 out of 24 patients completed 12-week follow-ups, with the rest having at least one follow-up assessment. The missing data were automatically handled by the linear mixed model in calculation of symptom change rate, as described in the manuscript.

Healthy subjects were recruited via advertisement from the nearby communities. The healthy participants received BPRS-A rating at baseline and at the 12th week. The fMRI scans were also performed at baseline. The exclusion criteria included: 1) lifetime history of any mood or psychotic

disorders as determined by SCID, non-patient version; 2) lifetime history of neurological disorders; 3) any serious non-psychiatric disorder that could affect brain functioning; 4) mental retardation; and 5) MR imaging contraindications.

Patients in the discovery sample and healthy individuals completed four fMRI paradigms during the scans: an eyes-closed resting state scan, a reward gambling task (2), an oddball task (3), and a multi-source interference task (MSIT) (4). Patients in the validation sample completed four fMRI paradigms as well, with two of the tasks different from the discovery sample (resting state, MSIT, finger tapping task, and competing response task).

Scan protocols

The discovery sample and the healthy subject sample were scanned with a 3T SIEMENS Prisma scanner using the Human Connectome Project (HCP) protocol (5). Specifically, the BOLD images were acquired with multi-band echo-planar imaging (EPI) sequence: TR = 720 ms, TE = 33 ms, FA = 52 degree, slice thickness = 2 mm, 72 continuous slices, FOV = 231*231 mm, voxel size = 2.2*2.2*2 mm, multi-band factor = 8. The high-resolution T1 structural images were acquired with the magnetization-prepared rapid gradient-echo (MP-RAGE) sequence: TR = 2400 ms, TE = 2.22 ms, FA = 8 degree, slice thickness = 0.8 mm, 208 continuous slices, FOV = 256*256 mm, voxel size = 0.8*0.8*0.8 mm. The resting-state scan was conducted with 2 runs of 7.2 min each, while the task scans varied between 5.8 and 15.6 min (MSIT: 4 runs of 3.9 min each; reward task: 2 runs of 2.9 min each; oddball task: 4 runs of 2.6 min each).

The validation sample was scanned with a 3T GE Signa scanner. The BOLD images were scanned with the following EPI sequence: TR = 2000 ms (with the exception of the MSIT task, TR = 1500 ms), TE = 30 ms, FOV = 240*240 mm, slice thickness = 3mm, 40 continuous slices, voxel size = 3.75*3.75*3 mm. T1 structural images were acquired with an inversion-recovery prepared 3D fast spoiled gradient (IR-FSPGR) sequence: TR = 7.5 ms, TE = 3 ms, TI = 650 ms, FOV = 240*240 mm, slice thickness = 1 mm, 216 continuous slices. The acquisition time was 5 min for resting state, 4.6 min for finger tapping task, 8.5 min for competing response task, and 13.4 min for MSIT (2 runs of 6.7 min each).

Image preprocessing

The discovery sample and the healthy subject sample were preprocessed with the Human Connectome Project (HCP) pipeline (6), including a total of five major steps (PreFreeSurfer, FreeSurfer, PostFreeSurfer, fMRI Volume, fMRI Surface). Briefly, images were corrected for gradient nonlinearity induced distortion, head motion, and phase-encoding related distortion, and then registered to individual T1 images and normalized to the Montreal Neurological Institute (MNI) space. The validation sample was preprocessed with the standard pipeline implemented in the SPM12 software (https://www.fil.ion.ucl.ac.uk/spm/software/spm12/), including slice timing correction, realignment for head motion, structural and functional image coregistration, and normalization to the MNI space. Finally, a 4-mm FWHM kernel was applied to the normalized images for spatial smoothing.

The preprocessed images were further scrutinized for head motion using the measure of frame-wise displacement (FD) as defined by Power et al. (7). Here, to mitigate motion-related effects and meanwhile maximize the sample size, we excluded subjects with an average FD larger than the group mean plus three times the standard deviation in the discovery sample. This led to the rejection of one patient, leaving a total of 48 patients for further analysis.

Construction of connectivity matrices

The construction of connectivity matrices followed our prior publications (8-10). After preprocessing, mean time series from each of the 300 nodes defined in the Seitzman atlas (11) were extracted. The extracted time series were further corrected for the effects of task-evoked coactivations (for task data), white matter, cerebrospinal, and global signals, 24 head motion parameters (i.e. 6 translational and rotational parameters, their first derivatives, and the squares of these 12 parameters), and FD. These noise-corrected time series were then temporally filtered with either band pass (rest data, 0.01-0.1 Hz) or high pass (task data, 0.01 Hz). Since each paradigm was scanned with multiple runs, we concatenated the time series from different runs for each paradigm, and subsequently used the concatenated time series to construct whole-brain connectome matrices. Specifically, a 300*300 connectivity matrix was computed by pairwise Pearson correlations for each subject during each fMRI paradigm. These matrices were further used for the cross-paradigm connectivity (CPC) analysis.

Estimation of subject-specific change rates

For the estimation of subject-specific change rates, all subjects' psychosis scores at all time points were entered into a linear mixed model in R as dependent variable, where time point was modelled as fixed variable and subject as random variable. In particular, the following model was fitted by maximizing the restricted log-likelihood, and individualized slopes were estimated and extracted from the model:

Score ~ time point + (1 + time point | subject)

Further explanation of the CPC approach

In this study, we used an approach termed "Cross-Paradigm Connectivity (CPC)" to combine fMRI data from multiple paradigms (8, 12), which essentially extracts shared components from connectivity matrices derived from different fMRI paradigms. The rationale of this approach is based on the previous findings that the human brain connectome constitutes an individual-unique, trait-like structure that is ubiquitously present across different fMRI paradigms, and the connectome architecture derived from a single paradigm is a mixture of such trait and state-related measures (13, 14). Therefore, the CPC approach was used with the aim of extracting such trait-like connectomic architecture for each subject.

It has increasingly been recognized in the literature that prediction with state-dependent, single-paradigm data will not achieve a comparable performance as the combined multi-paradigm data in which more trait-like variations are examined (12, 15, 16). In our prior study (12), we have shown the improvement of predictability as a function of paradigm quantity. Therefore, we have included

all of the four available paradigms in the dataset and used the CPC approach to conduct the prediction analysis, aiming to boost the prediction performance as much as possible.

Supplementary Results

The CPC matrices captured individualized "trait" connectome

We have previously published a series of studies showing that the CPC matrices could capture the vast majority of shared variance across the connectivity matrices constructed from different fMRI paradigms at the individual level (8-10, 12). Here we further confirmed these findings in the present data. In particular, the CPC matrices in the discovery sample explained about 70% of shared variance across the four paradigms (mean 71.5±4.6), and the CPC matrices in the validation sample explained about 60% of shared variance (mean 58.6±4.3), suggesting that the derived CPC matrices do reflect individualized "trait" organizations of the functional connectome.

The predictive model was not driven by any specific paradigm

Since the CPC matrices captures the state-independent organizations in the human connectome, the derived predictive model should not be driven by any specific fMRI paradigm. To verify this, we further extracted the 14 final features from each of the original single-paradigm connectivity matrices in the discovery sample and calculated their associations with symptom change rates during each paradigm. We found significant correlations for all of the four paradigms (positive features: $r > 0.49$, $P < 0.001$; negative features: $r < -0.52$, $P < 0.001$), which suggests that the derived predictive model is not driven by any specific paradigm, and the selected features are correlated with treatment response in a state-independent way.

The prediction performance was not driven by head motion

Head motion is an important consideration in imaging studies. While we have carefully controlled head motion during data analysis, here we further tested whether the derived prediction results would relate to head motion. For this we calculated the Pearson correlations between the predictors (i.e. sum of the 5 positive features or 9 negative features) and individual mean FDs in both samples. The results did not show any significant associations between predictors and FDs (discovery sample: $r < 0.14$, $P > 0.16$; validation sample: $r < 0.001$, $P > 0.99$). These findings suggest that the reported prediction performance is unlikely to be driven by head motion.

The prediction performance was not driven by duration of untreated psychosis (DUP)

The DUP has been shown to be a strong predictor for treatment response in psychosis (17, 18). In this study, only part of the subjects had the DUP data and therefore we did not include DUP as a covariate in the predictive model. However, this raises the possibility that the derived predictors may simply reflect DUP differences among patients. To rule out this possibility, we calculated the Pearson correlations between the predictors and DUP in patients with available data. No significant correlations between predictors and DUP were found in both samples (discovery sample: $r > -0.11$,

$P > 0.57$; validation sample: $r > -0.11$, $P > 0.60$), suggesting that the prediction performance is unlikely to be driven by DUP.

The model was not predictive of time- and practice-related effects

To exclude the possibility that the model was simply predictive of time- and practice-related effects during the experiment, we additionally estimated the prediction performance in a sample of 28 healthy subjects (mean age 28.2 y, 13 males). Similar to patients, the healthy subjects received baseline fMRI scans and were followed up for 12 weeks. The BPRS-A ratings were conducted for each individual at the baseline and at the 12th week. Here, no significant changes were shown for psychosis scores over time in healthy subjects (slope = 0.01, $P = 0.26$). When applying the same model to healthy subjects, we did not observe a significant predictive effect on symptom change (r *[predicted vs observed]* = 0.05, $P = 0.38$), suggesting that our findings are not simply predictive of time-related effects.

Prediction performance with different thresholds

One tuning parameter in the CPM analysis is the initial threshold for feature selection (for the present results we used $P < 0.0005$ as described in the manuscript). To test the prediction performance across different thresholds, we repeated the analysis with a range of thresholds from $P < 0.001$ to $P < 0.01$. We found that the in-sample prediction performance (within the discovery sample) remained stable across different thresholds (~0.40, Table S2); however, the out-of-sample performance (validation sample) significantly decreased with the increase of P value, suggesting that a more lenient initial threshold may introduce noise and therefore reduce generalizability.

Prediction performance with each single fMRI paradigm

To further verify that the combination of multiple fMRI paradigms would improve the prediction performance, we additionally examined the prediction performance with each single fMRI paradigm used in the two datasets. The results demonstrated that single paradigm had considerably lower performance compared with the combined data, both in the discovery sample and in the validation sample. While direct comparison between paradigms needs to be cautious given the differences in scan length, these findings nevertheless suggest that inclusion of multiple fMRI paradigms would benefit the prediction performance for clinical response studies.

Prediction performance after removal of individuals with mood disorders

While it is unclear whether the neural signatures of antipsychotic response in mood disorders with psychosis would be different from those in schizophrenia spectrum disorders, we additionally tested the performance of the same 14 features in the discovery sample after excluding individuals with mood disorders (three with bipolar and three with depression). We found very similar associations of the positive and negative feature scores with symptom change rates (positive: $r = 0.83$; negative: $r = -0.79$). Applying the trained model to the validation sample demonstrated very similar prediction performance (r *[predicted vs observed]* = 0.47). These findings suggest that our observed prediction performance is transdiagnostically similar among individuals with psychosis.

Prediction performance for each single drug

While the sample size for each treatment group is rather small (see Table 1), we did not train predictive models for each drug separately, and therefore the reported findings may reflect a mixed effect of both drugs. However, in order to test whether the prediction performance could be similar between the two drugs, we additionally examined the effects of our identified predictors separately for each drug group. In the discovery sample, there were strong associations between the feature scores and symptom change rates in both groups, with the effect slightly larger among individuals treated with aripiprazole (risperidone: r = 0.74 for positive features and r = -0.72 for negative features; aripiprazole: r = 0.95 for positive features and r = -0.87 for negative features). When applying the predictive model to the validation sample, the risperidone group showed a prediction performance of *r [predicted vs observed]* = 0.58 and the aripiprazole group showed a prediction performance of *r [predicted vs observed]* = 0.44. This suggests that our prediction model is suitable for both drugs. Since the sample size for single drugs is very small, the results need to be interpreted with great caution. Future cohort studies with large patient sample targeting a single drug effect are certainly warranted.

Prediction performance in people with and without cannabis use

Since cannabis use is common among patients with psychosis, we additionally tested the prediction performance separately for people with and without cannabis use disorder. Here, 23 out of 48 patients in the discovery sample and 10 out of 24 patients in the validation sample were simultaneously diagnosed with cannabis use disorder. In the discovery sample, slightly higher associations were detected between the feature scores and slopes among people without cannabis use (positive features: r = 0.89; negative features: r = -0.85) compared with those with cannabis use (positive features: r = 0.74; negative features: r = -0.62). Applying the trained model to the validation sample revealed a prediction performance of *r [predicted vs observed]* = 0.56 among those without cannabis use and *r [predicted vs observed]* = 0.39 among those with cannabis use. These supplementary findings suggest that the identified predictors may show better performance among patients without cannabis use. Notably, this is consistent with our prior work that cannabis use could dampen the performance of the previously reported striatal connectivity predictors (19).

Test of the identified predictors in dichotomized response groups as defined by Sarpal et al. (1)

Notably, in this study the clinical outcome was evaluated by individualized slope coefficients, which essentially quantify averaged change rates for each subject across the 12-week follow-up time. This is different from a dichotomous outcome measure (responder/non-responder) as used in Sarpal et al. (1). In order to test whether our identified features would also distinguish different response groups defined in that study, we dichotomized our samples based on the same criteria. Specifically, an individual was considered as a responder if he/she had a score of 3 (mild) or less for all psychosis items in the BPRS-A on at least two consecutive time points (or on only one time point if total follow-up time less than 4 weeks). Here, 35 out of 48 patients in the discovery sample and 17 out of 24 patients in the validation sample were assigned to the responder group, with others assigned to the non-responder group.

Using two-sample t test to compare the summed feature scores between the two groups, we observed significant differences for both positive and negative features in the discovery sample (positive: P = 0.001, negative: $P < 0.001$). However, such differences did not generalize to the validation sample ($P >$ 0.25 for both positive and negative features), suggesting that the identified connectomic predictors in the present study may not be a generalizable neural marker for the previously defined response/non-response status.

Associations of the present predictors with those reported in Sarpal et al. (1)

We also tested whether the present predictors were correlated with the previously reported striatal connectivity findings. To this end, we calculated the striatal connectivity index (SCI) based on Sarpal et al. (1) and correlated the individualized SCI with our positive and negative feature scores in the discovery sample. We found non-significant correlations between these two findings (r = 0.16, P = 0.27 for positive features and r = -0.22, P = 0.13 for negative features), suggesting that these two findings may capture different variations in treatment response and therefore may have complementary values in clinical response studies (prediction of individualized change rate vs prediction of predefined response group).

Data reanalysis with a different paradigm-combination approach

Besides the CPC, there have been other alternative approaches in the literature to combine multiple fMRI paradigms, one of which is termed "general functional connectivity" (20). This approach combines paradigms by directly concatenating their time series. Here, we additionally tested the prediction performance by using this alternative approach. Our findings showed overall lower in-sample and out-of-sample performance with this approach (discovery sample: median *r [predicted vs observed]* = 0.34; validation sample: *r [predicted vs observed]* = 0.25, MSE = 0.022), suggesting that our CPC approach may show a superiority in the context of treatment prediction.

Predicting slopes calculated by simple linear regression model

By using linear mixed model, individual slopes were calculated by partial pooling towards the group-level fixed effect. While this would reduce noise and increase confidence of the estimated slopes, especially in small samples, it nevertheless may lead to a potential issue of "data leakage" during cross validation (CV). Ideally, when combining CPM and mixed model, one would need to estimate slopes separately for the training and testing samples to avoid this problem, and therefore a large sample size is required to obtain robust slope measures for both training data and testing data. However, given the small sample in this study, only n∼5 subjects were assigned to the test sample during each CV cycle, rendering the estimated slopes very unstable. To mitigate the potential "data leakage" problem, we here conducted a supplementary analysis, where we recalculated each individual's slope with a simple linear regression model in the discovery sample, thereby avoiding interdependency of slopes between individuals. We then tested the prediction performance using the same predictors and parameters for these new slope estimates. The result showed a prediction performance *r[predicted vs observed]* = 0.43, which was very similar to our original finding in the discovery sample (r = 0.41). In addition, since our findings were also tested in a completely independent sample (note that in the validation sample, slopes were estimated with a separate LME

model and therefore were completely independent of the discovery sample), they together suggest that the reported prediction performance is unlikely to be simply driven by data leakage.

Table S1. List of finally selected features in the discovery sample. The nodes and their belonged networks are defined by Seitzman et al. (11)

	Connection	**Belonged network**
Positive features		
1	L. supplementary motor – R. precuneus	CON – DMN
2	R. cerebellum lobule 4&5 – R. superior temporal	SMN – AN
3	R. cerebellum lobule 7b – R. lingual	FPN – VN
4	R. cerebellum lobule 6 – L. superior frontal	VN – DMN
5	R. inferior occipital – anterior cingulate	VN – DMN
Negative features		
1	R. rolandic operculum – R. postcentral	AN – SMN
2	R. supplementary motor – L. inferior frontal	CON – FPN
3	R. precuneus – L. precuneus	DMN – DMN
4	R. insula – R. putamen	AN – SMN
5	R. superior temporal – R. middle temporal	VAN – VAN
6	L. cerebellum crus 1 – R. cerebellum crus 1	SN – SN
7	R. precuneus – R. posterior cingulate	DMN – DMN
8	L. inferior temporal – R. orbitofrontal	DMN – DMN
9	R. cerebellum crus 1 – L. anterior cingulate	FPN – DMN

AN = auditory network; VN = visual network; SMN = sensorimotor network; SN = salience network; DMN = default-mode network; CON = cingular-opercular network; FPN = fronto-parietal network; VAN = ventral attention network.

Table S2. Prediction performance with different feature selection thresholds.

	Discovery sample		**Validation sample**		**Number of features**	
Initial threshold	***Median r***	***P***	***r***	***P***	***Positive***	***Negative***
$P < 0.0005$	0.41	0.01	0.47	0.01	5	9
$P < 0.001$	0.42	0.007	0.15	0.26	16	17
$P < 0.005$	0.40	0.004	0.28	0.08	117	78
$P < 0.01$	0.40	0.002	0.26	0.10	220	158

Table S3. Prediction performance with each single fMRI paradigm. Each row represents an fMRI paradigm used in the discovery sample, with the columns showing its in-sample median performance and out-of-sample validation performance with fMRI paradigms in the validation sample.

Discovery sample	**In-sample median *r***	**Validation sample *r***			
		Rest	**MSIT**	**CompResp**	**FingerTap**
Rest	0.45	0.18	0.19	0	0.19
MSIT	0.23	0.33	0.18	0	0
Oddball	0.33	0	0	0.02	0
Reward	0.35	0	0.05	0.23	0.28

Figure S1. Distributions of model performance (*r*[predicted vs observed]) from 100 repeats of the CPM analysis in the discovery sample. The blue histogram presents the distribution calculated from the original CPC matrices, and the yellow histogram presents the distribution after removing the identified 14 connections.

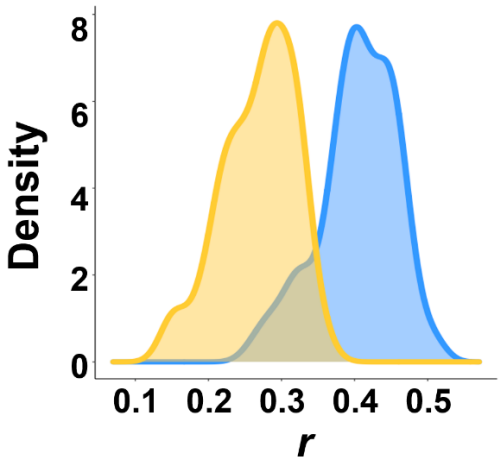

References

1. Sarpal DK, Argyelan M, Robinson DG, Szeszko PR, Karlsgodt KH, John M, Weissman N, Gallego JA, Kane JM, Lencz T, Malhotra AK. Baseline Striatal Functional Connectivity as a Predictor of Response to Antipsychotic Drug Treatment. Am J Psychiatry. 2016;173:69-77.
2. Barch DM, Burgess GC, Harms MP, Petersen SE, Schlaggar BL, Corbetta M, Glasser MF, Curtiss S, Dixit S, Feldt C, Nolan D, Bryant E, Hartley T, Footer O, Bjork JM, Poldrack R, Smith S, Johansen-Berg H, Snyder AZ, Van Essen DC, Consortium W-MH. Function in the human connectome: task-fMRI and individual differences in behavior. Neuroimage. 2013;80:169-189.
3. Ardekani BA, Choi SJ, Hossein-Zadeh GA, Porjesz B, Tanabe JL, Lim KO, Bilder R, Helpern JA, Begleiter H. Functional magnetic resonance imaging of brain activity in the visual oddball task. Brain Res Cogn Brain Res. 2002;14:347-356.
4. Bush G, Shin LM. The Multi-Source Interference Task: an fMRI task that reliably activates the cingulo-frontal-parietal cognitive/attention network. Nat Protoc. 2006;1:308-313.
5. Van Essen DC, Ugurbil K, Auerbach E, Barch D, Behrens TE, Bucholz R, Chang A, Chen L, Corbetta M, Curtiss SW, Della Penna S, Feinberg D, Glasser MF, Harel N, Heath AC, Larson-Prior L, Marcus D, Michalareas G, Moeller S, Oostenveld R, Petersen SE, Prior F, Schlaggar BL, Smith SM, Snyder AZ, Xu J, Yacoub E, Consortium W-MH. The Human Connectome Project: a data acquisition perspective. Neuroimage. 2012;62:2222-2231.
6. Glasser MF, Sotiropoulos SN, Wilson JA, Coalson TS, Fischl B, Andersson JL, Xu J, Jbabdi S, Webster M, Polimeni JR, Van Essen DC, Jenkinson M, Consortium W-MH. The minimal preprocessing pipelines for the Human Connectome Project. Neuroimage. 2013;80:105-124.
7. Power JD, Barnes KA, Snyder AZ, Schlaggar BL, Petersen SE. Spurious but systematic correlations in functional connectivity MRI networks arise from subject motion. Neuroimage. 2012;59:2142-2154.
8. Cao H, Chén OY, Chung Y, Forsyth JK, McEwen SC, Gee DG, Bearden CE, Addington J, Goodyear B, Cadenhead KS, Mirzakhanian H, Cornblatt BA, Carrión RE, Mathalon DH, McGlashan TH, Perkins DO, Belger A, Seidman LJ, Thermenos H, Tsuang MT, van Erp TGM, Walker EF, Hamann S, Anticevic A, Woods SW, Cannon TD. Cerebello-thalamo-cortical hyperconnectivity as a state-independent functional neural signature for psychosis prediction and characterization. Nat Commun. 2018;9:3836.
9. Cao H, Ingvar M, Hultman CM, Cannon T. Evidence for cerebello-thalamo-cortical hyperconnectivity as a heritable trait for schizophrenia. Transl Psychiatry. 2019;9:192.
10. Cao H, Zhou H, Cannon TD. Functional connectome-wide associations of schizophrenia polygenic risk. Mol Psychiatry. 2021;26:2553-2561.
11. Seitzman BA, Gratton C, Marek S, Raut RV, Dosenbach NUF, Schlaggar BL, Petersen SE, Greene DJ. A set of functionally-defined brain regions with improved representation of the subcortex and cerebellum. Neuroimage. 2020;206:116290.
12. Cao H, Chen OY, McEwen SC, Forsyth JK, Gee DG, Bearden CE, Addington J, Goodyear B, Cadenhead KS, Mirzakhanian H, Cornblatt BA, Carrión RE, Mathalon DH, McGlashan TH, Perkins DO, Belger A, Thermenos H, Tsuang MT, van Erp TGM, Walker EF, Hamann S, Anticevic A, Woods SW, Cannon TD. Cross-paradigm connectivity: reliability, stability, and utility. Brain Imaging Behav. 2021;15:614-629.

13. Cole MW, Bassett DS, Power JD, Braver TS, Petersen SE. Intrinsic and task-evoked network architectures of the human brain. Neuron. 2014;83:238-251.
14. Finn ES, Shen X, Scheinost D, Rosenberg MD, Huang J, Chun MM, Papademetris X, Constable RT. Functional connectome fingerprinting: identifying individuals using patterns of brain connectivity. Nat Neurosci. 2015;18:1664-1671.
15. Finn ES, Scheinost D, Finn DM, Shen X, Papademetris X, Constable RT. Can brain state be manipulated to emphasize individual differences in functional connectivity? NeuroImage. 2017;160:140-151.
16. Finn ES. Is it time to put rest to rest? Trends in Cognitive Sciences. 2021;25:1021-1032.
17. Perkins DO, Gu H, Boteva K, Lieberman JA. Relationship between duration of untreated psychosis and outcome in first-episode schizophrenia: a critical review and meta-analysis. Am J Psychiatry. 2005;162:1785-1804.
18. Marshall M, Lewis S, Lockwood A, Drake R, Jones P, Croudace T. Association between duration of untreated psychosis and outcome in cohorts of first-episode patients: a systematic review. Arch Gen Psychiatry. 2005;62:975-983.
19. Blair Thies M, DeRosse P, Sarpal DK, Argyelan M, Fales CL, Gallego JA, Robinson DG, Lencz T, Homan P, Malhotra AK. Interaction of Cannabis Use Disorder and Striatal Connectivity in Antipsychotic Treatment Response. Schizophr Bull Open. 2020;1:sgaa014.
20. Elliott ML, Knodt AR, Cooke M, Kim MJ, Melzer TR, Keenan R, Ireland D, Ramrakha S, Poulton R, Caspi A, Moffitt TE, Hariri AR. General functional connectivity: Shared features of resting-state and task fMRI drive reliable and heritable individual differences in functional brain networks. Neuroimage. 2019;189:516-532.